Chapter 3. Development of Nanocomposite by Magnetic Field Induced Alignment of GNP

The contents of this chapter have appeared as:

A. Tiwari, S.K. Panda, Magnetic field induced alignment of graphene nanoplatelets in epoxy resin to develop model nanocomposite, ***J. Compos. Mater***. 57 (15) (2023) 2451–2466. https://doi.org/10.1177/00219983231172063.

3.1. Introduction

In this research, to strengthen the magnetic characteristics of the GNP, we considered that magnetite Fe_3O_4 nanoparticles are decorated on the GNP surfaces and dispersed the nanoparticle in the epoxy. Then, the nanoparticles and epoxy mixture are subjected to a weak DC magnetic field to fabricate aligned nanocomposites. Furthermore, we proposed a mathematical model based on magnetophoretic (MAP) and classical hydrodynamics that describes all of the physical phenomena during the alignments process of Fe_3O_4-GNP in epoxy during curing under the applied DC electromagnetic (as shown in **Fig. 3.4)**. The procedure developed gets rid of many an ambiguity of approximation with scientific validation. The reproducibility of the results can be confirmed, as these mathematical models are well-established and affirmed by proper sketches and microstructural analysis. To the best of our knowledge, this is the first work that studied and compared the time required to align the GNP and Fe_3O_4-GNP as well as optimised the alignment influencing parameters in epoxy under the weak magnetic field as a consequence of aligning Fe_3O_4-GNP nanoparticles.

3.2. Method: Physical phenomena of applied DC electromagnetic-coerced alignment of Fe_3O_4-GNP

In the developed method, two sets of differential equations are used to combine the contributions of MAP and classical hydrodynamics. The equations could explain the rotational motion of nanoparticles as well as the chaining phenomena caused by a weak DC magnetic field. As well, the migration phenomena that become relevant towards the south pole of the

applied magnetic fields is also included, while in the absence of magnetic fields, slackening of the nanoparticles network is caused by Brownian motion. Furthermore, an attempt has been made to properly integrate specific contributions and then evaluation of the required time to complete all dynamic mechanisms in the creation of Fe_3O_4-GNP networks in epoxy suspension during curing under the presence and absence of a DC electromagnetic field. One important objective of the model is the optimization of the process parameters (i.e., DC magnetic fields, magnetic properties of nanoparticles, and epoxy viscosity) for the fabrication of a fully cured epoxy nanocomposite with an aligned Fe_3O_4-GNP employing DC electromagnetic fields and comparing the alignment time for GNP and Fe_3O_4-GNP. In fact, each of the aforementioned phenomena has a different response duration, and a correct assessment of them leads to the fabrication of a nanocomposite with highly aligned Fe_3O_4-GNP, with no migration toward the south pole of the magnet and network relaxation with a low magnetic field. Mathematical model is used to compare how long it takes for GNP and Fe_3O_4-GNP to align in epoxy under optimum influencing parameters. elucidated with adequate sketches, is to explain a theoretical description of the classical dynamics of all mechanisms that occur during the alignment phenomenon of Fe_3O_4-GNP nanoparticles under the applied DC electromagnetic field and as a result of multiple external body forces. Mathematical models for determining the time required to complete each mechanism are also proposed.

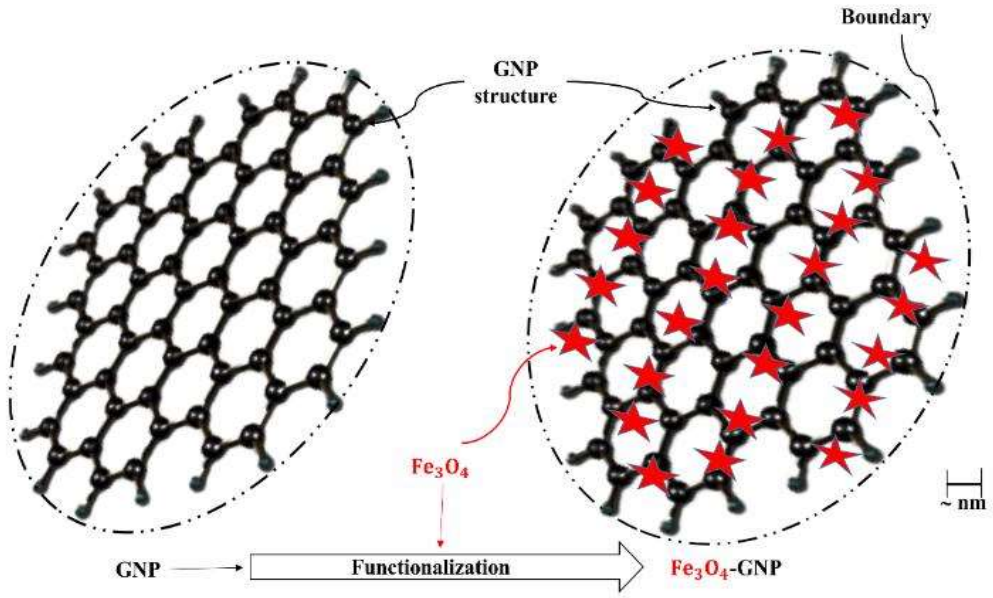

Fig. 3.1. Shows the schematic illustration of graphene nanoplatelets (GNP) and functionalized GNP with magnetic nanoparticles Fe3O4 i.e., Fe_3O_4-GNP

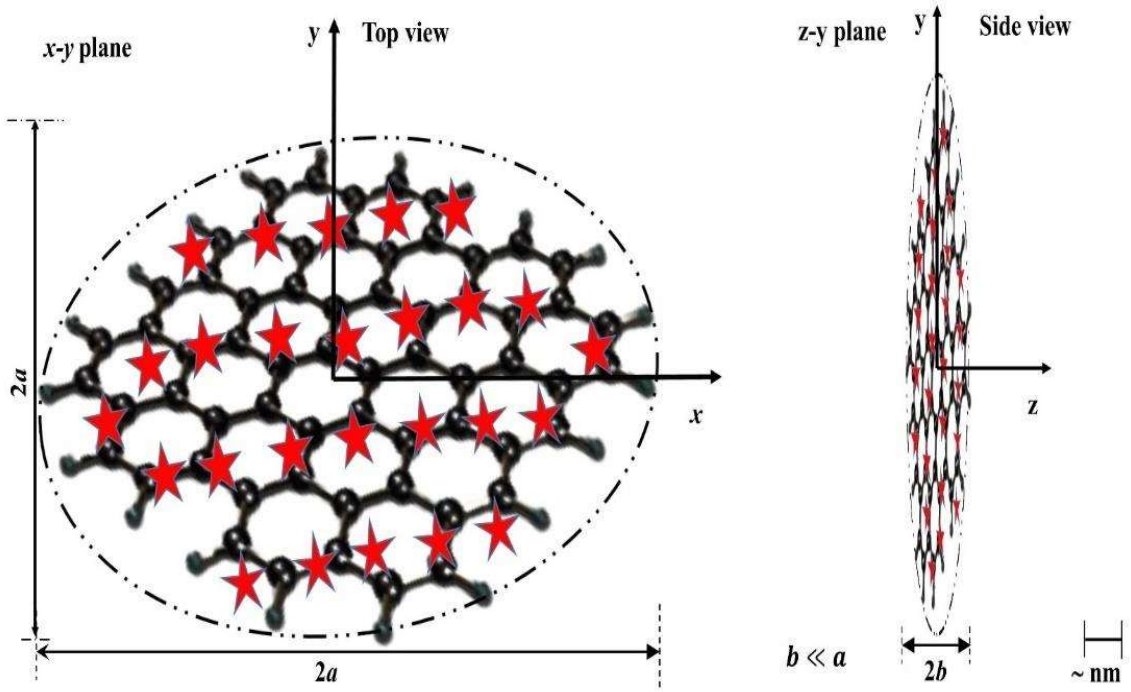

Fig. 3.2. Visualizes the Fe_3O_4-GNP as the shape of an oblate spheroid and also denotes equatorial radius '*a*' as well as the distance '*b*' from the centre to pole along the symmetry axis of the Fe_3O_4-GNP.

We assume a suspension of identical, rigid, neutrally buoyant axisymmetric Fe_3O_4-GNP nanoparticles that is dilute (in the sense that particle-particle hydrodynamic interactions can be ignored). Brownian effects are prominent since the nanoparticles are in the submicron range. Variations in the ambient velocity gradient are thought to occur on a macroscopic length scale that would be much relatively large than the particle size. We focus on constant gradients for simplicity, but our method can easily be expanded to time-dependent.

As a foundation for this model, several hypotheses were proposed. The GNP was modelled as a rigid oblate spheroid with equatorial radius 'a' and the distance from centre to pole along the symmetry axis '$\bar{b}$'. As illustrated in **Fig. 3.1**, Fe_3O_4 magnetic nanoparticles are evenly decorated

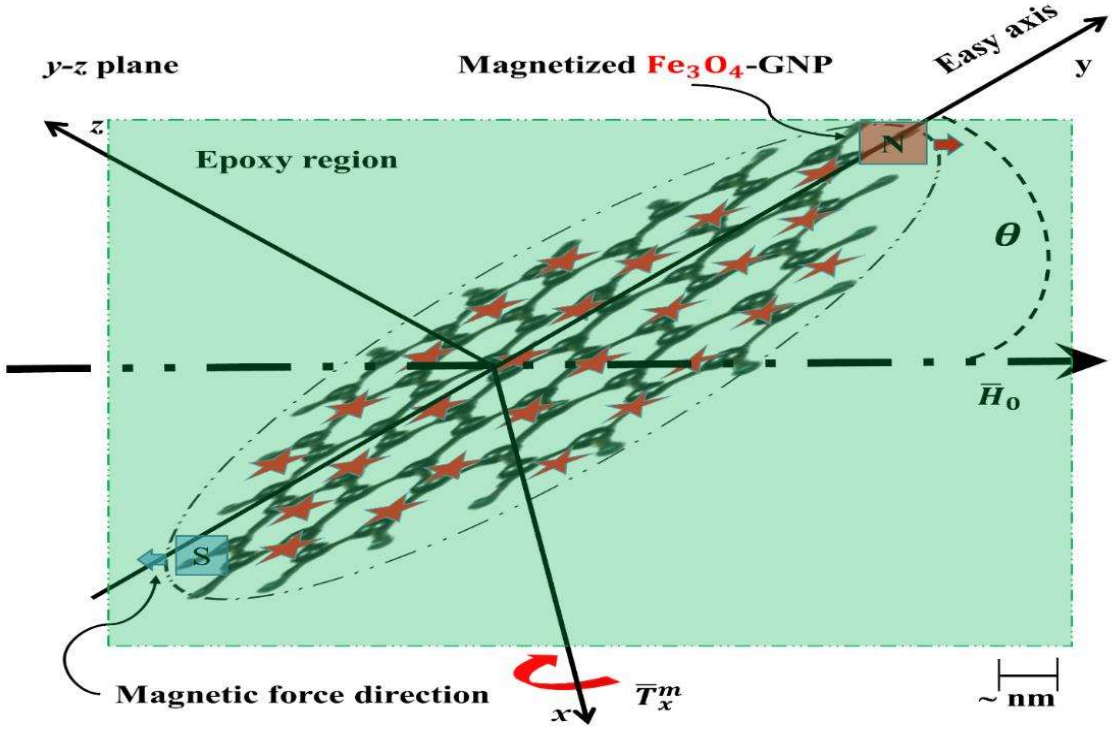

Fig. 3.3. Displays the angle 'θ' between the direction of applied magnetic field '$\bar{H}_0$' and easy axis of Fe_3O_4-GNP as well as the induced magnetic torque about x-axis '$\bar{T}_x^m$' on the dispersed Fe_3O_4-GNP in epoxy.

on the surfaces of GNP, and these decorated materials are referred to as functionalized GNP, or Fe_3O_4-GNP, and have the ability to magnetise like super ferromagnetic. While the shape of the Fe_3O_4-GNP as shown in **Fig. 3.2**, is like as GNP and the length (equatorial diameter) of the

Fe_3O_4-GNP is clearly analogous to that of neat GNP, but its thickness (Designated as *'b')* is larger than neat GNP '$\bar{b}$' due to the Fe_3O_4 decoration.

3.2.1. Rotation of Fe_3O_4-GNP particles

In the absence of magnetic fields, the inherent magnetic moments of Fe_3O_4 are randomly oriented thereby neutralising the net effect and as a result, the net magnetization is zero. In the presence of a suitable homogeneous magnetic field, however, the magnetic field induces forces on the Fe_3O_4-GNP, resulting in induced net magnetic moments. All the magnetic moments are now oriented in parallel, resulting in a sufficient number of induced dipolar magnetic moments. This phenomenon is known as MAP, which is responsible for the angular and translation motion of the Fe_3O_4-GNP (**Fig. 3.3** and **Fig. 3.4**'s first step shows it schematically). Accordingly, the magnetic moments are obtained to conquer any hydrothermal motion and rotate to attain the equilibrium state.

Under the homogeneous DC electromagnetic fields, the Fe_3O_4-GNP are suspended in an epoxy medium with magnetic permeability $\mu_m \approx \mu_0$,[150]. The applied DC magnetic field ($\overline{H}_0$) induced magnetic intensity within the Fe_3O_4-GNP ($\overline{H}^-$) and which developed effective dipole magnetic moment $\overline{m}_{\text{eff}}$, that is defined by the linear constitutive law[151];

$$\overline{m}_{\text{eff}} = V\overline{H}^- = V\bar{\chi}_V \bullet \overline{H}_0 \tag{3.1}$$

where, $V(= 4\pi a^2 b/3)$ and $\bar{\chi}_V$ are volume and tensor magnetic effective volume susceptibility of Fe_3O_4-GNP. The ellipsoidal particle's geometrical axisymmetry leads us to believe that the x, y, and z -axes correspond to the principal crystalline axes. The reciprocity and principal crystalline axes condition permits that $\bar{\chi}_{V,xy} = \bar{\chi}_{V,yz} = \bar{\chi}_{V,zx} = 0$. Within Fe_3O_4-GNP, the induced magnetic intensity is defined as;

$$\overline{H}^- = \left\{ \frac{C_x}{1 + \bar{\chi}_{V,xx} L_{xx}} \hat{x} + \frac{C_y}{1 + \bar{\chi}_{V,yy} L_{yy}} \hat{y} + \frac{C_z}{1 + \bar{\chi}_{V,zz} L_{zz}} \hat{z} \right\} \overline{H}_0 \tag{3.2}$$

here L_{xx}, L_{yy} and L_{zz} are the depolarization factor along the respective axis of the ellipsoidal. The relationship between these is denoted as;

$$\begin{cases} 0 \leq L_{xx}, L_{yy}, L_{zz} \leq 1 \\ L_{xx} + L_{yy} + L_{zz} = 1 \end{cases} \tag{3.3}$$

According to the above equation, all of the factors are positive. As a result, the induced effective dipole moment vector $\overline{m}_{\text{eff}}$ is deduced;

$$\overline{m}_{\text{eff}} = V \left\{ \frac{\bar{\chi}_{V,xx} C_x}{1 + \bar{\chi}_{V,xx} L_{xx}} \hat{x} + \frac{\bar{\chi}_{V,yy} C_y}{1 + \bar{\chi}_{V,yy} L_{yy}} \hat{y} + \frac{\bar{\chi}_{V,zz} C_z}{1 + \bar{\chi}_{V,zz} L_{zz}} \hat{z} \right\} \bar{H}_0 \tag{3.4}$$

where $C_x, C_y$and C_z are the magnetic field components' direction cosines. The magnetic alignment torque "$\overline{T}^m$" is represented in **Fig. 3.3** and expressed as;

$$\begin{aligned} \overline{T}^m &= \mu_0 (\overline{m}_{\text{eff}} \times \bar{H}_0) \\ &= \mu_0 V \left\{ \frac{\bar{\chi}_{V,xx} C_x}{1 + \bar{\chi}_{V,xx} L_{xx}} \hat{x} + \frac{\bar{\chi}_{V,yy} C_y}{1 + \bar{\chi}_{V,yy} L_{yy}} \hat{y} + \frac{\bar{\chi}_{V,zz} C_z}{1 + \bar{\chi}_{V,zz} L_{zz}} \hat{z} \right\} \\ &\times \left\{ \frac{C_x}{1 + \bar{\chi}_{V,xx} L_{xx}} \hat{x} + \frac{C_y}{1 + \bar{\chi}_{V,yy} L_{yy}} \hat{y} + \frac{C_z}{1 + \bar{\chi}_{V,zz} L_{zz}} \hat{z} \right\} \bar{H}_0^2 \end{aligned} \tag{3.5}$$

According to Eq (3.5), torque would rotate the Fe_3O_4-GNP nanoparticles to achieve the equilibrium condition, i.e., the minimum energy condition. When any of its crystalline principal axes is aligned with the direction of applied magnetic fields ($\bar{H}_0$) during rotation, then equilibrium is attained. However, stability is only achieved when the particles' longest crystalline principal axis aligns parallel to the applied field's direction, and the longest crystalline axis is referred to as the specific easy axis of the particles. According to Eq (3.5), the x-component of magnetic alignment torque is responsible for paralleling the easy axis with the magnetic field, i.e.

$$\bar{T}_x^m = V \mu_0 \left[\frac{(\bar{\chi}_{V,yy} - \bar{\chi}_{V,zz}) + \bar{\chi}_{V,yy} \bar{\chi}_{V,zz} (L_{zz} - L_{yy})}{\left(1 + \bar{\chi}_{V,yy} L_{yy}\right)\left(1 + \bar{\chi}_{V,zz} L_{zz}\right)} \right] \bar{H}_0^2 C_y C_z \tag{3.6}$$

The magnetic field is applied in the y-z plane, with the easy axis forming an angle θ with its vector. According to authors [152,153], the depolarization factor $L_{xx} = L_{yy} \ll 1$ and $L_{zz} \approx 1$ for very thin oblate spheroids. The **Fig. 3.2** revealed that $\bar{\chi}_{V,yy}$ and $\bar{\chi}_{V,zz}$ are the values parallel and perpendicular to the particle's easy axis, respectively, and can be written as $\bar{\chi}_{V,yy} = \bar{\chi}_{V,\text{II}}$ and $\bar{\chi}_{V,zz} = \bar{\chi}_{V,\perp\perp}$. Using the condition, Bates [151]defined the torque as follows:

$$\bar{T}_x^m = \bar{T}^m = V\mu_0 \left[\bar{\chi}_{V,\text{II}} - \bar{\chi}_{V,\perp\perp}\right] \bar{H}_0^2 C_y C_z = \frac{2\pi a^2 b \mu_0 H_0^2}{3} \bar{\chi}_{V,a} \sin 2\theta \tag{3.7}$$

where $\bar{\chi}_{V,a} = \bar{\chi}_{V,\text{II}} - \bar{\chi}_{V,\perp\perp}$ is the volume anisotropic susceptibility. The magnetic nanoparticles have a positive volume anisotropic susceptibility $\bar{\chi}_{V,a}$ value, implying that the easy axis of the Fe_3O_4-GNP nanoparticles attempting to orient parallel to the applied magnetic field. During the rotation, the Fe_3O_4-GNP must counteract the hydrodynamic torque $\bar{T}^H$, which is induced by drag originates by the suspension medium, i.e. epoxy. The hydrodynamic torque is defined as[154,155]

$$\bar{T}^h = -\eta k_r \frac{d\theta}{dt} \tag{3.8}$$

where the η, k_r and $\frac{d\theta}{dt}$ are represent the dynamic viscosity of the epoxy, the rotational friction coefficient of the particle's geometry, i.e. oblate spheroids $k_r = 32a^3/3$ [155], and the angular velocity of the particles, respectively. Consider the dynamic condition, which is provided by the torque balance $\bar{T}^m = \bar{T}^h$:

$$\frac{d\theta}{dt} = -\xi \sin 2\theta \tag{3.9}$$

The Eq. (3.9) can be readily integrated as follows:

$$\theta(t) = \tan^{-1}\left(\tan \theta_i e^{-\xi t}\right) \tag{3.10}$$

where: $\xi = \frac{\pi}{16}\frac{b}{a}\frac{\mu_0 \bar{H}_0^2}{\eta} \bar{\chi}_{V,a}$.

The Eq.(3.10) may conveniently be used to calculate the amount of time required to get from the initial angular position of the easy axis (θ_i) to a generic angular position θ w.r.t magnetic field:

$$t_r(\theta) = \frac{1}{\xi} \ln \frac{\tan \theta_i}{\tan \theta} \tag{3.11}$$

The influence of the initial angular orientation on the required time for alignment can be analysed utilising Eq.(3.11). In fact, the final angular position θ_f would be equal to zero at complete alignment (ideal state), and the accompanying time $t_r(\theta_f)$ would be indefinite. So after, the final angular position θ_f was set to slightly above zero ($\theta_f \approx 1.0^{\circ}$) to prevent unnecessary the asymptotic time. The rotating time can be calculated as

$$t_r(\theta_f) = \frac{1}{\xi} \ln \frac{\tan \theta_i}{\tan \theta_f} \tag{3.12}$$

Thus according Eq. (3.12), the rotating time of Fe_3O_4-GNP nanoparticles is directly proportional to the epoxy's dynamic viscosity, aspect ratio of functionalized GNP, and inversely proportional to the particles' volume anisotropic susceptibility of the Fe_3O_4-GNP.

3.2.2. Chaining of Fe_3O_4-GNP nanoparticles

Because the magnetized Fe_3O_4-GNP nanoparticles have opposite poles, they have strong attractive magnetic forces as soon as the Fe_3O_4-GNP particles rotated. This can be assessed analytically by taking into consideration both the attractive magnetic force and the translational viscous force owing to the Fe_3O_4-GNP nanoparticles' translation motion and this phenomenon causes end-to-end connection of the nanoparticles. **Fig. 3.4** depicts it schematically.The time required for this chaining phenomena can be estimated. The equivalent magnetic pole strength at the ends of the Fe_3O_4-GNP nanoparticles was quantified utilising induced magnetic torque as scaler products of the magnetic pole strength at the ends of the particles and the diameter of the ellipsoid (i.e. the distance of 2*a*) as follows:

$$\overline{T}^{m} = m * \mu_0 \overline{H}_0 * 2a \sin\theta \tag{3.13}$$

Even though both torques, Eq. (3.7) and (3.13) have the same magnitude and direction, we determined the magnetic pole strength at the particles' ends as.

$$m = \frac{2\pi ab\overline{H}_0}{3} \overline{\chi}_{V,a} \cos\theta \tag{3.14}$$

Thus, the adjacent Fe_3O_4-GNP nanoparticles having unlike magnetic poles attracted each to other. The attracting magnetic force is defined as:

$$F_m = \frac{\pi(ab)^2 \overline{H}_0^2}{9\mu_0 . r^2} \left(\overline{\chi}_{V,a}\right)^2 \cos^2\theta \tag{3.15}$$

where r is the end to end distance between two unlike poles of the Fe_3O_4-GNP nanoparticles. Due to magnetic torque on the particles, the easy axis of the particles is aligned parallel to the applied magnetic field. Thus, the

final angular position (θ_f) w.r.t magnetic field is $\theta_f = \theta \approx 0$. Now the attracting force is rewritten as:

$$F_m = \frac{\pi(ab)^2 \overline{H}_0^2}{9\mu_0 . r^2} \left(\overline{\chi}_{V,a}\right)^2 \tag{3.16}$$

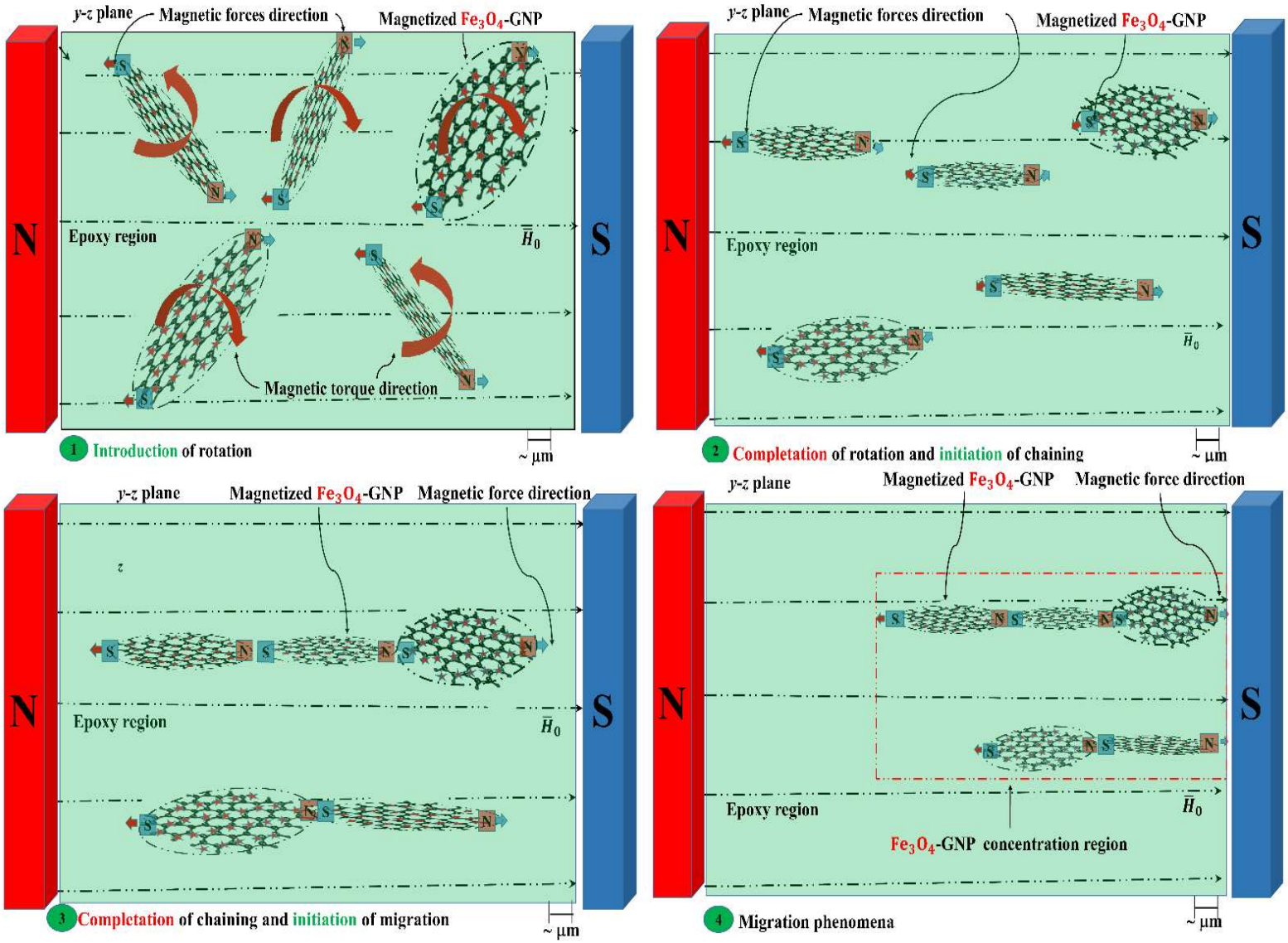

Fig. 3.4. Illustrates the orientation mechanism of the Fe_3O_4-GNP (a) Initiation of rotation. (b) Completion of rotation and initiation of chaining. (c) Completion of chaining and initiation of migration (d) Migration phenomena.

Because translational viscous friction opposes the motion of the Fe_3O_4-GNP nanoparticles, the attractive forces cause translational motion in the epoxy. At equilibrium, the shear force $-\eta k_t \frac{dr}{dt}$ and magnetic force Eq (3.16) are equal and opposite, resulting in:

$$-\eta k_t \frac{dr}{dt} = \frac{\pi(ab)^2 \overline{H}_0^2}{9\mu_0 . r^2} \left(\overline{\chi}_{V,a}\right)^2 \tag{3.17}$$

where the term $'k_t'$ is defined [156] for oblate spheroid as geometric constant that is known as the translational friction coefficient. This constant is expressed as

$$k_t = 6\pi(a^2 b)^{1/3} \frac{\sqrt{|(b/a)^2 - 1|}}{\tan^{-1}\left(\frac{\sqrt{|(b/a)^2 - 1|}}{(b/a)}\right)} \tag{3.18}$$

The Eq. (3.17)can be used to derive the translational motion equation as follows:

$$\frac{dr}{dt} = -\frac{\lambda}{r^2} \tag{3.19}$$

where: $\lambda = \frac{\pi(ab)^2 \overline{H}_0^2}{9\eta k_t \mu_0} \left(\overline{\chi}_{V,a}\right)^2$

The solution of differential Eq (3.19 is given as:

$$r(t) = \sqrt[3]{-3\lambda t + r_i} \tag{3.20}$$

where r_i is the initial end to end distance between two unlike poles of the adjacent nanoparticles. Once end to end to connection is completed i.e., $r(t) = 0$, then the expected time to complete this connection (i.e. $r(t) = 0$) is determined as:

$$t_c(r_i) = \frac{r_i^3}{3\lambda} \tag{3.21}$$

The initial end to end distance r_i between two unlike poles of the adjacent Fe_3O_4-GNP nanoparticles can be estimated by applying analogous technique as used by[125]. The initial distance be controlled by content of the Fe_3O_4-GNP nanoparticles in matrix. Considering the

dispersion of the particles in the entire matrix is uniform and the associated volume $\hat{V}$ for the single nanoparticles:

$$\hat{V} = \frac{1}{\rho}\frac{m_n}{w_n} \tag{3.22}$$

where ρ , w_n, and m_n are the density of epoxy, weight fraction of the Fe_3O_4-GNP nanoparticles and mass of each Fe_3O_4-GNP nanoparticles, respectively. The associated volume $\hat{V}$ can be modelled as a square-based parallelepiped, having its base edges are equal to equatorial diameter ($2a$) of the Fe_3O_4-GNP nanoparticles and its height is equal to the average of the initial end to end distance (r_i) between two unlike poles of the adjacent particles as shown in **Fig. 3.5**. In this case, we constrain the motion of the nanoparticles with only three degrees of freedom

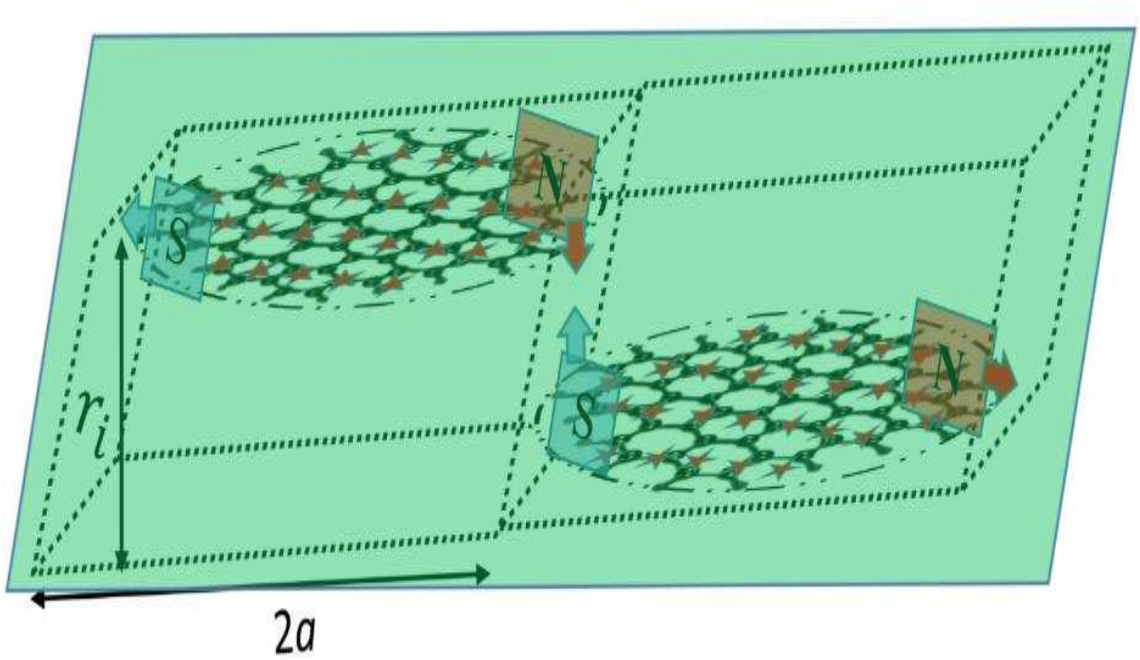

Fig. 3.5. Shows the schematic representation of the volume associated with a single Fe_3O_4-GNP nanoparticle after the orientation in the magnetic field direction.

(one rotation and two translational motion) and the average of the initial end to end distance (r_i) between two unlike poles of the Fe_3O_4-GNP nanoparticles can be calculated by Eq.(3.22):

$$r_i = \frac{\hat{V}}{4a^2} = \frac{1}{\rho}\frac{m_n}{w_n}\frac{1}{4a^2} \tag{3.23}$$

3.2.3. Migration of Fe_3O_4-GNP nanoparticles

The DC electromagnetic field applied to the Fe_3O_4-GNP–epoxy colloid encourages migration toward the north poles under magnetophoretic mobility, indicating the presence of north poles (N) on the Fe_3O_4-GNP nanoparticles. When the Fe_3O_4-GNP nanoparticles are close enough to the electromagnetic south poles (P), they aggregate onto the south poles (P). The Fe_3O_4-GNP nanoparticles' north poles (N) and south poles (P) combined together produce extremely potent magnetic fields that can be used to attract additional Fe_3O_4-GNP nanoparticles. Consequently, ramified Fe_3O_4-GNP nanoparticle network structures may be seen from the south poles. The final step of **Fig. 3.4** depicts it schematically. The Fe_3O_4-GNP nanoparticles concentration is considerably biased toward the south poles (P), because there's no such thing as a homogeneous system. U_m, the magnetophoretic mobility of nanoparticles, is calculated by using the following[157,158]:

$$U_m = \frac{v_m x}{\mu_0 \bar{H}_0^2} = \frac{\bar{\chi}_{V,a} V}{6\pi \eta a} \tag{3.24}$$

where v_m is terminal migration velocity of the nanoparticles and x is migration distance of the particles.

The Eq. (3.24) can give the migration time t_m for migration distance x_m by the nanoparticles:

$$t_m = \frac{9}{2}\frac{x_m^2}{ab}\frac{\eta}{\mu_0 \bar{H}_0^2 \bar{\chi}_{V,a}} \tag{3.25}$$

According to Eq. (3.25) migration time is proportional to epoxy system viscosity and migration distance, whereas migration distance is inversely proportional to geometric parameter and volume anisotropic susceptibility of the Fe_3O_4-GNP nanoparticles, as well as the applied magnetic field strength.

3.2.4. Slackening of aligned Fe_3O_4-GNP nanoparticles

As shown in **Fig. 3.6**, in the absence of DC electromagnetic fields, slackening has become an unpreventable incidence. When Brownian diffusion becomes important for motion, it has a tendency to reduce the alignment and chain network of nanoparticles. The slackening

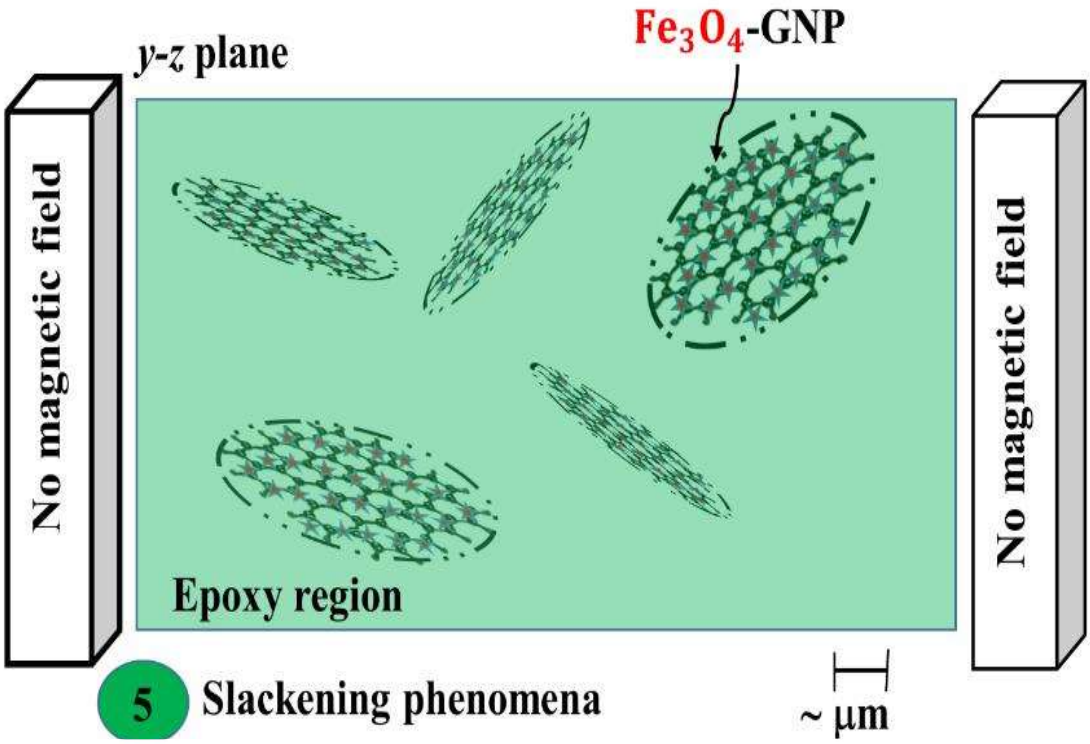

Fig. 3.6. Illustrates the slackening of Fe_3O_4-GNP nanoparticles after removal of magnetic fields.

phenomenon causes the Fe_3O_4-GNP nanoparticles' orientation and chain-like structures to fade together.

The slacken angle θ_{s-r} about x-axis ensues through time t_{s-r},which is known as slacken rotation time, is related by[156,157,159]:

$$t_{s-r} = \frac{4\pi\eta a^3 K_s}{k_B T}\langle\theta_{s-r}^2\rangle \tag{3.26}$$

where k_B and T are the Boltzmann constant and the epoxy temperature, respectively. While K_s is an ellipsoidal form factor given by [160]:

$$K_s = \frac{4e^3(2-e^2)}{3(-2e+(1+e^2)\ln([1+e]/[1-e]))} \quad \text{and} \quad \mathrm{e} = \sqrt{1-\left(\frac{b}{a}\right)^2} \tag{3.27}$$

Furthermore, as rotational slackening begins, the Fe_3O_4-GNP nanoparticles are subjected to translational diffusion. The following equation describes the relationship between slacken translation time t_{s-t} and mean squared slacken displacement $\langle x_{s-t}^2 \rangle$ as:

$$t_{s-t} = \frac{6\pi\eta a}{2k_B T(\ln(a/b)-0.3)} \langle x_{s-t}^2 \rangle \tag{3.28}$$

3.3. Experimental section

In this work, a most common thermosetting polymer for polymer composite, DGEBA based epoxy resin (LY-556) was considered as matrix. As catalyst, hardener Aradur (HY-951) procured from Huntsman, Hyderabad was consumed as curing agent. The stoichiometric quantities of the matrix and curing agent was taken 10:1 by weight. The GNP used as nanoparticles reinforcement is obtained from XG Sciences, USA. The GNP is composed of teeny piles of graphene sheets having a platelet shape. The particles diameter and thickness of the GNP are in micron and nanometres range, respectively. The Fe_3O_4 nanoparticle was synthesized via solvo-thermal reaction and preparation of GNP epoxy and Fe_3O_4-GNP epoxy nanocomposites with complete characterisations of the nanoparticle along with nanocomposites are explained in the second part of this paper. A rheometer MCR302 (Anton Paar, Austria) with parallel plate attachment was used to determine dynamic chemorheological characteristics of epoxy during curing process. The Viscosity test were conducted at room temperature (30°C) in dynamic strain sweep (rotary) mode, with shear rate 50 s^{-1}. To study the magnetic characteristics, magnetic hysteresis loops were recorded at room temperature (300 K) using a Vibrating Sample Magnetometer (Quantum Design, USA). A weak magnetic field was applied to a liquid mixture of Fe_3O_4-GNP and epoxy that included 0.05 wt % of Fe_3O_4-GNP, and the

alignment of the Fe_3O_4-GNP before curing and after curing was observed using a dewinter optical microscope.

3.4.Results and discussion

3.4.1. Experimental results

Fig. 3.7 illustrates the chemorheological curve of the used reactive system during an isothermal test at 30^0 C. The viscous nature of the epoxy resin and hardener mixture can be observed over time. The viscosity of the reactive system increases with time, but the initial increase in viscosity of epoxy is very gradual up to 15 minutes, after which the increment of the viscosity of these increases exponentially. It is clear that the viscosity of the epoxy rapidly increases after 30 minutes. Following that, a gelation process occurs, which prevents the solution from flowing. Finally, it can be concluded that the ideal casting time is ranged from 15 to 30 minutes.

The magnetic hysteresis of the nanoparticles was measured at ambient temperature in a magnetic field that was applied and swept from -1T to 1T. **Fig. 3.8** depicts magnetic properties of GNP, Fe_3O_4 and Fe_3O_4-GNP. The details of magnetic properties of the nanoparticles are summarised in the

Table 3.1. Tiny remanence and coercivity were present in the magnetic hysteresis of Fe_3O_4-GNP, indicating soft ferrimagnetic behaviour of it. It appears that the Fe_3O_4-GNP has soft magnetic characteristics which was critical for magnetic alignment application. This characterization study demonstrates that Fe_3O_4-GNP exhibits superparamagnetic behaviour as a result of Fe_3O_4 attachments to the GNP surfaces.

Fig. 3.9 depicts optical microscope pictures of the Fe_3O_4-GNP/epoxy microstructure (0.05 wt %) in the presence of a weak magnetic field. The images are taken at before curing, as well as after the curing process. As anticipated, Fe_3O_4-GNP in the epoxy changes orientation over time and aligns with the direction of the applied magnetic field. The majority of the Fe_3O_4-GNP in

the most recent images are positioned nearly parallel to the applied magnetic field. We demonstrated that aligning the Fe_3O_4-GNP in an epoxy resin using a very low magnetic field can be a successful substitute for doing so with a large magnetic field. Many a practical

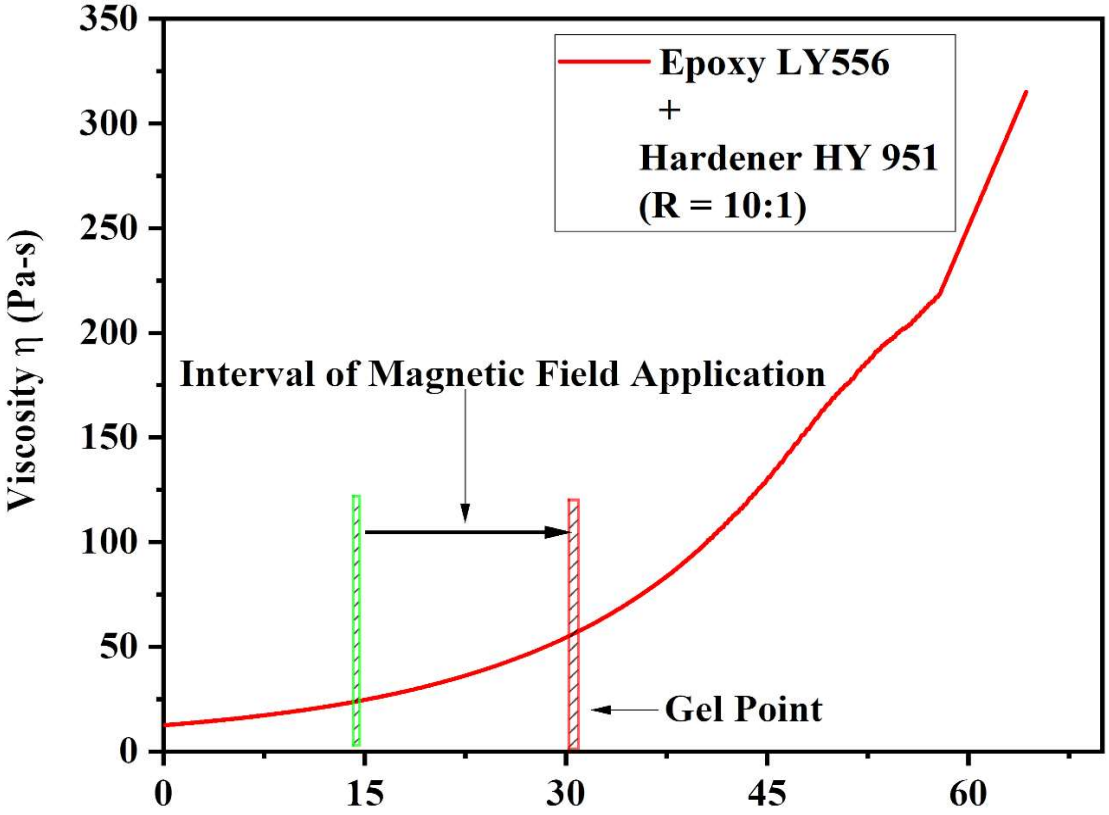

Fig. 3.7. Shows chemorheological behaviours of Epoxy LY-556 and Hardener HY-951 with ratio 10:1 during curing process

mechatronics and electrical devices, high magnetic field seems impractical and limits the utility of the equipment for the GNP base functional materials

Table 3.1.Magnetic properties of nanoparticles.

Nanoparticles	Magnetic properties at (300K, 40Hz)							
	M_s (emu/gm)	H_s (T)	M_r (emu/gm)	H_c (T)	Mass magnetic susceptibility (χ) (emu/gm-T)			
					$\overline{H}_0$=0.05 T	$\overline{H}_0$=0.1 T	$\overline{H}_0$=0.15 T	$\overline{H}_0$=0.2 T
GNP	~ 00	~ 00	~ 00	~ 00	~ 00	~ 00	~ 00	~ 00
Fe_3O_4	81	0.95	3.689	0.0049	536.11	223.48	84.06	38.20
Fe_3O_4-GNP	16	0.85	0.944	0.0044	76.81	20.27	8.53	6.49

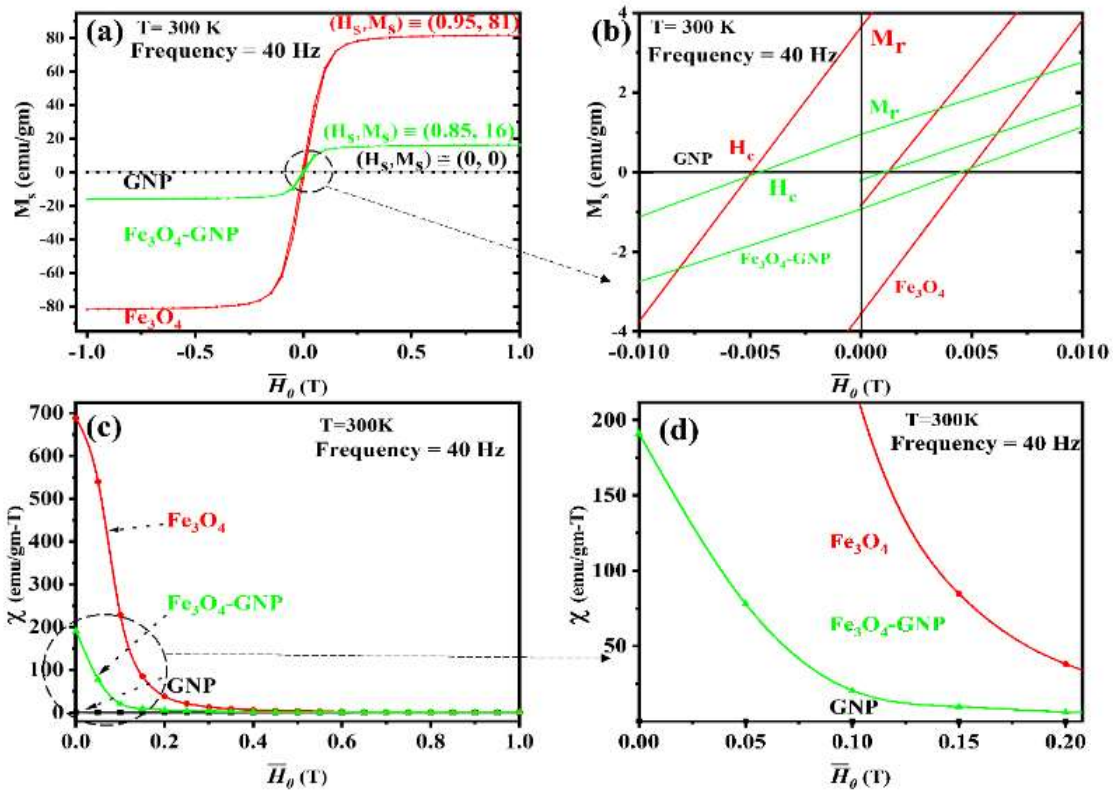

Fig. 3.8. Shows the (a) saturation magnetization (Ms) vs. applied Magnetic field ($\overline{H}_0$) having details the characteristics of coercivity and remanence, while (b) demonstrates the mass magnetic susceptibility(χ) vs. applied magnetic field ($\overline{H}_0$) of Fe_3O_4-GNP.

3.5.Model Results

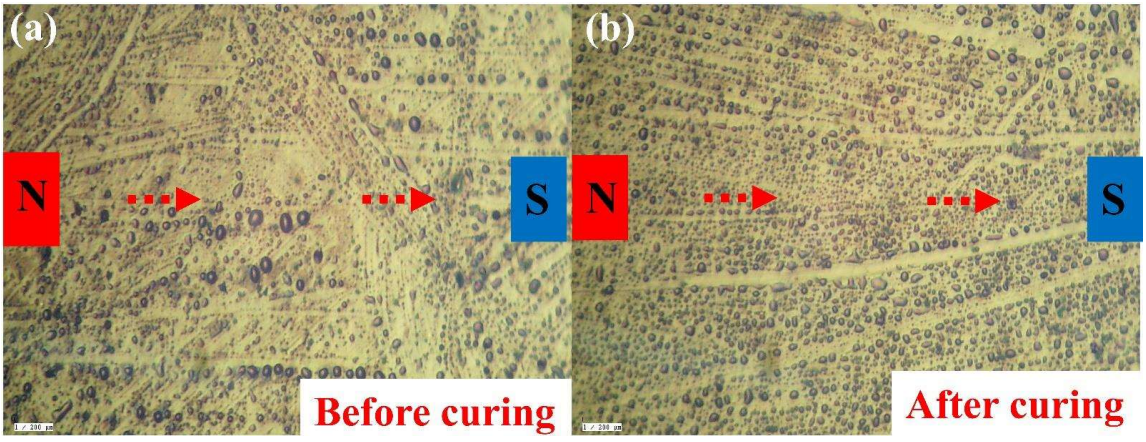

Fig. 3.9. show the optical microscope images of the Fe_3O_4-GNP before and after curing in the epoxy under the weak magnetic field.

In order to align the GNP and Fe_3O_4-GNP in the liquid epoxy in the direction of the applied magnetic field prior to the epoxy gelling, the ideal time and magnetic field can be determined

using the mathematical model discussed in section 3.2. The GNP, Fe_3O_4-GNP, and epoxy characteristics as specified in Table 3.2

Table 3.2 were used to obtain all model predictions. In order to optimise the results, the

Symbol	Expression (Unit)	Symbol	Expression (Unit)
a	1.75x10-7(m)	T	300 (K)
$\overline{b}$	25x10-9(m	μ	4 x π x 10-7 (N/A2)
b	45x10-9(m)	k_B	1.38064852 × 10-23 (m2 kg s-2 K-1)
w_n	0.05x10-2	ρ	1175 (kg/m3)

viscosity of the epoxy during the curing process, the volume magnetic susceptibility, and the applied magnetic field were varied. The variational influence on the amount of time needed for the alignment process is examined below.

Table 3.2 Parameters for mathematical model

Symbol	Expression (Unit)	Symbol	Expression (Unit)
a	$1.75x10^{-7}$(m)	T	300 (K)
$\overline{b}$	$25x10^{-9}$(m	μ	4 x π x 10^{-7} (N/A^2)
b	$45x10^{-9}$(m)	k_B	1.38064852 × 10^{-23} (m^2 kg s^{-2} K^{-1})
w_n	$0.05x10^{-2}$	ρ	1175 (kg/m^3)

3.5.1. Rotation

Rotation is the most important alignment-related behaviour. Eq.(3.11) evaluates the rotating phenomenon in order to optimise the rotation time by varying the initial angle, epoxy viscosity, magnetic field, and volume magnetic susceptibility time to complete rotation in the magnetic field direction.

Fig. 3.10. shows the time as a function of the initial angle of the GNP and Fe_3O_4-GNP nanoparticle in the epoxy with respect to the magnetic field direction during the alignments process, for various values of epoxy viscosity at the constant applied magnetic field $\overline{H}_0 = 0.05$ T. For the same situation, the GNP rotation time is significantly higher than the Fe_3O_4-

GNP rotation time. Because the epoxy takes less time to gel than GNP does to rotate, the time needed for GNP alignments is not adequate for casting. Most often this has been the challenge to restrict the wide scale application of nanocomposites in structural applications. This resulted in the conclusion that the attachment of Fe_3O_4 nanoparticle to GNP is favourable to lower the rotation time for the minimum applied magnetic field i.e $\overline{H}_0 = 0.05$ T. Another author who used the electric field for carbon nanotube alignments discovered similar results[161].

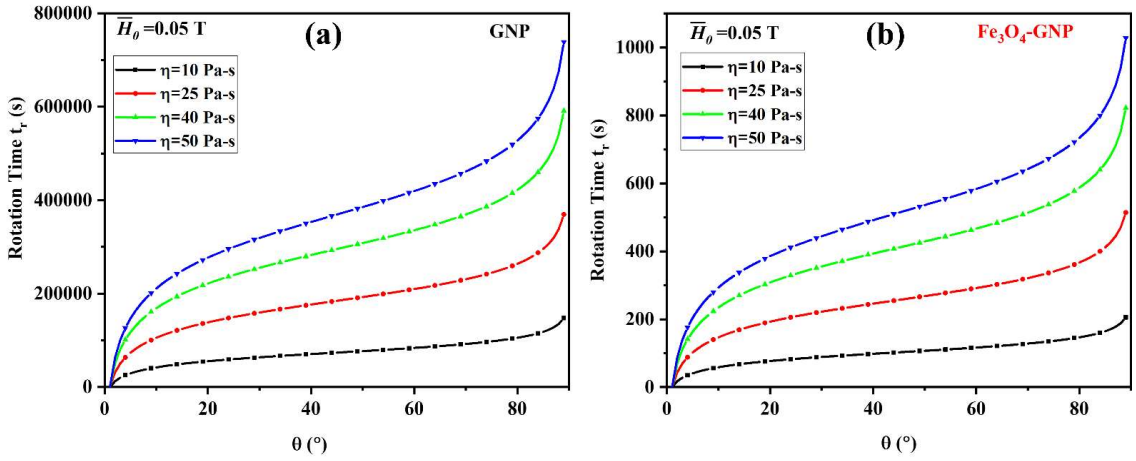

Fig. 3.10. Shows the plots of the alignment time of the (a) GNP and (b) Fe_3O_4-GNP as a function of the initial angle θ^0 for the rotational motion.

The rotating periods needed for GNP and Fe_3O_4-GNP nanoparticles are compared in **Fig. 3.11**., which also demonstrates how the magnetic field and viscosity affect this time when other variables are maintained constant. It has been shown, how the magnetic field affects the rotation time of nanoparticles for various epoxy viscosity levels throughout the alignment procedure. We came to the conclusion that the GNP was inadequate for alignment under the circumstances because it required more rotating time than Fe_3O_4-GNP based on the trend of the plot. The Fe_3O_4-GNP can be said to rotate in a magnetic field direction with a very low magnetic field, $\overline{H}_0 = 0.05$ T at a viscosity of 40 Pa-s, however the low magnetic field is inadequate to rotate the GNP within the epoxy system's gel time.

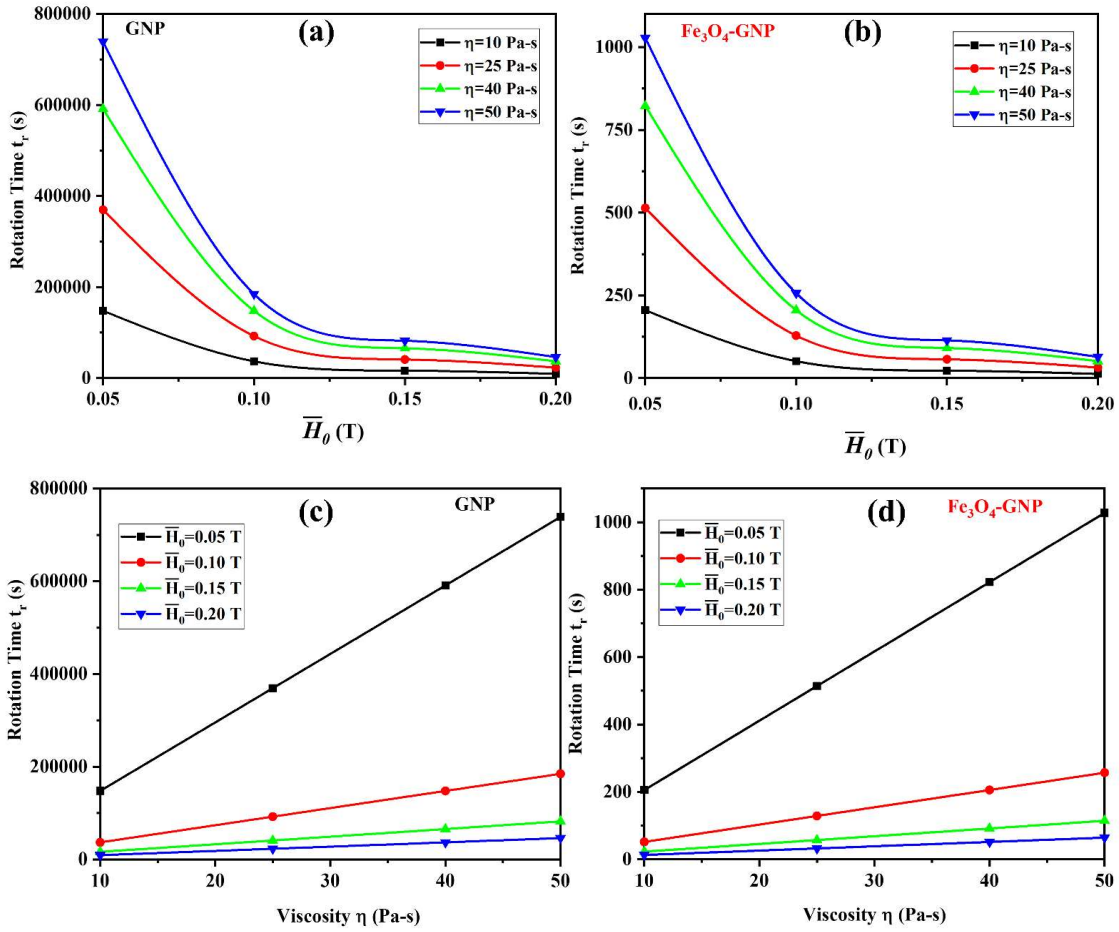

Fig. 3.11. shows the influence of the magnetic field and viscosity on the rotational time of (a) and (c) GNP, (b) and (d) Fe_3O_4-GNP.

3.5.2. Chaining of nanoparticles

The opposite poles of the magnetised nanoparticles attract each other thereby translating and forming a chain like structure, after the nanoparticles are rotated in a magnetic direction, which is modelled by Eq. (3.21). The significance of these events is utmost during alignments. **Fig. 3.12** depicts the time required by this process under various magnetic fields that are applied and with varying epoxy viscosities. Using the same parameter, the graph shows that Fe_3O_4-GNP links faster than GNP nanoparticles. This implies that under these conditions, alignment time with the GNP is not acceptable. The sum of the rotating and chaining times is near to or equal

to the gelation time of the epoxy for Fe_3O_4-GNP. It is best to use the alignments' parameters $\overline{H}_0 = 0.05$ T and η=40 Pa-s.

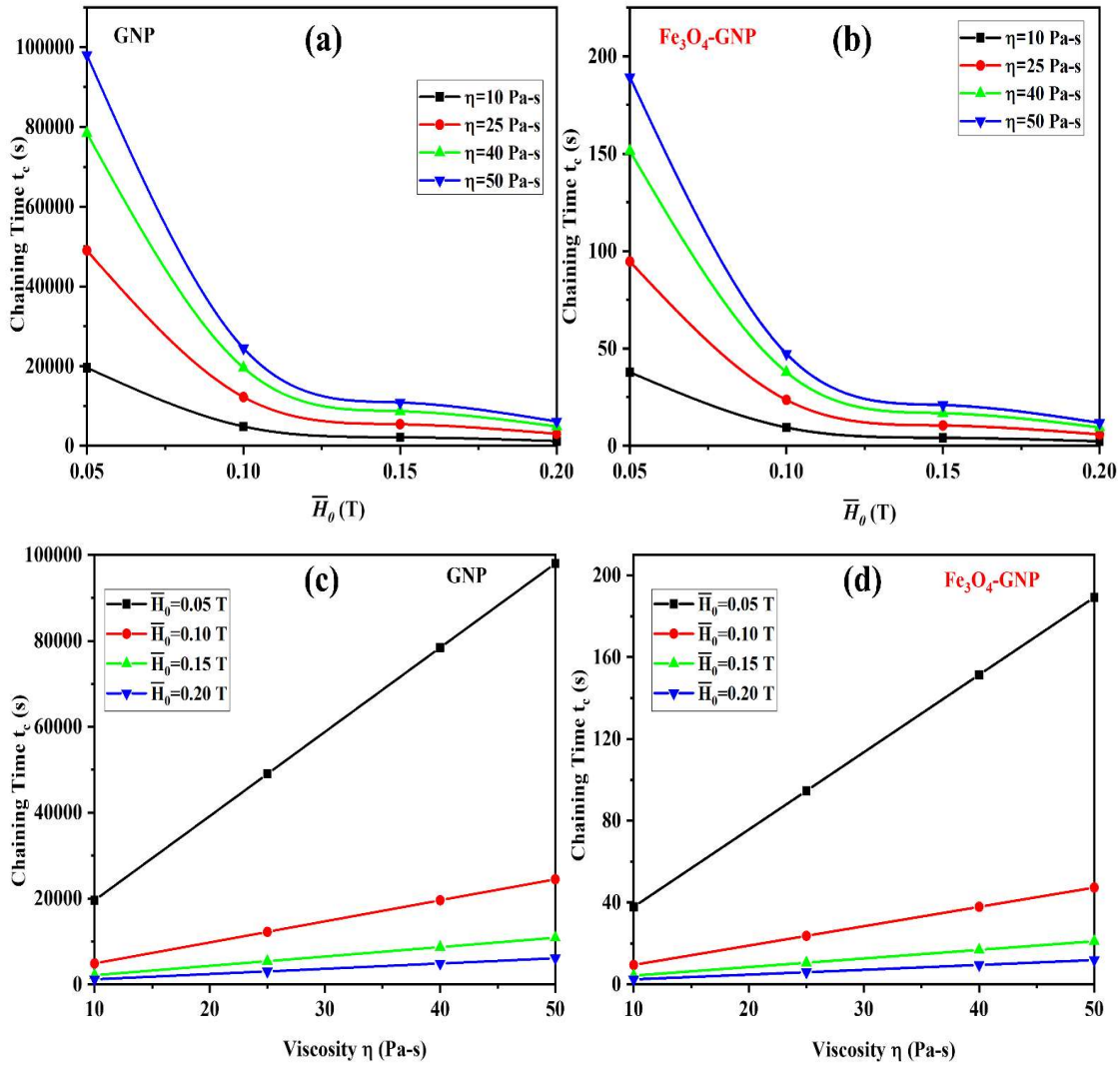

Fig. 3.12. shows the influence of the magnetic field and viscosity on the chaining time of (a) and (c) GNP, (b) and (d) Fe_3O_4-GNP.

3.5.3. Migration

Eq. (3.25) calculates the time expected for GNP and Fe_3O_4-GNP nanoparticles to migrate a distance for a particular set of conditions, which is influenced by their magnetophoretic mobility. The migration distance x_m between the poles was fixed to 1 mm in order to assess the order of magnitude on the time scale of the migration phenomena t_m. **Fig. 3.13** shows the behaviour of the time variation with magnetic field and viscosity of the epoxy. The plot's trend demonstrates how the migration time changes exponentially with magnetic field variation at constant viscosity, whereas the time variation is linear with changing viscosity at constant magnetic field. For the same field and viscosity conditions as earlier, the migration times of Fe_3O_4-GNP and GNP nanoparticles are studied. Compared to the migration time for GNP, the

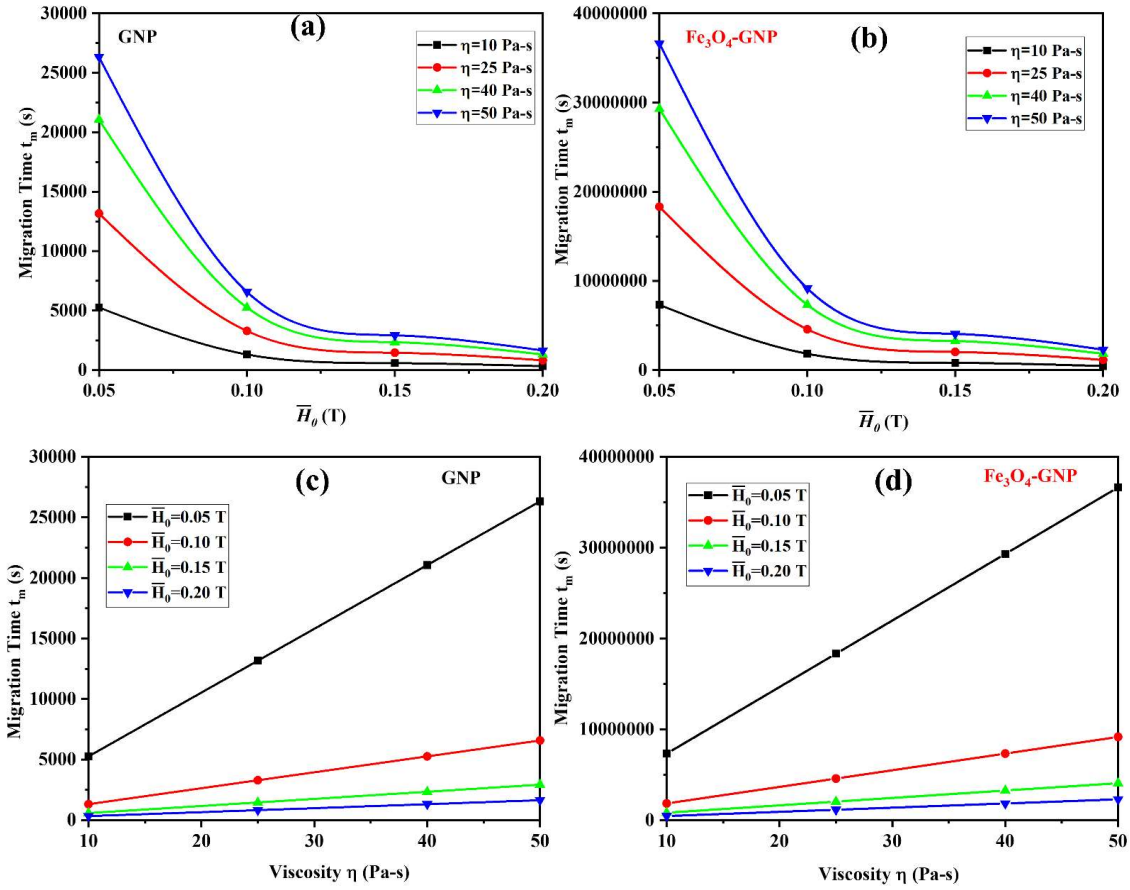

Fig. 3.13. demonstrates how the magnetic field and viscosity affect the migration time of (a) and (c) GNP, (b) and (d) Fe_3O_4-GNP.

migration time of the Fe_3O_4-GNP is significantly higher. Because the epoxy had already gelled

before the migration time, the migration time was noticeably higher than the epoxy gel point, suggesting that there was hardly any possibility of a migration mechanism occurring during the alignment process.

3.5.4. Slackening

The slackening mechanism illustrated by the Eq. (3.26) and (3.28) represents the rotational and translational slackening time, respectively. **Fig. 3.14** delineates how the relaxation times increase linearly with viscosity. More specifically, rotational slackening requires more time to complete than translational slackening. Since the conductive network is disrupted when the faster relaxation mechanism occurs, this factor is taken into consideration when calculating the system's relaxation time.

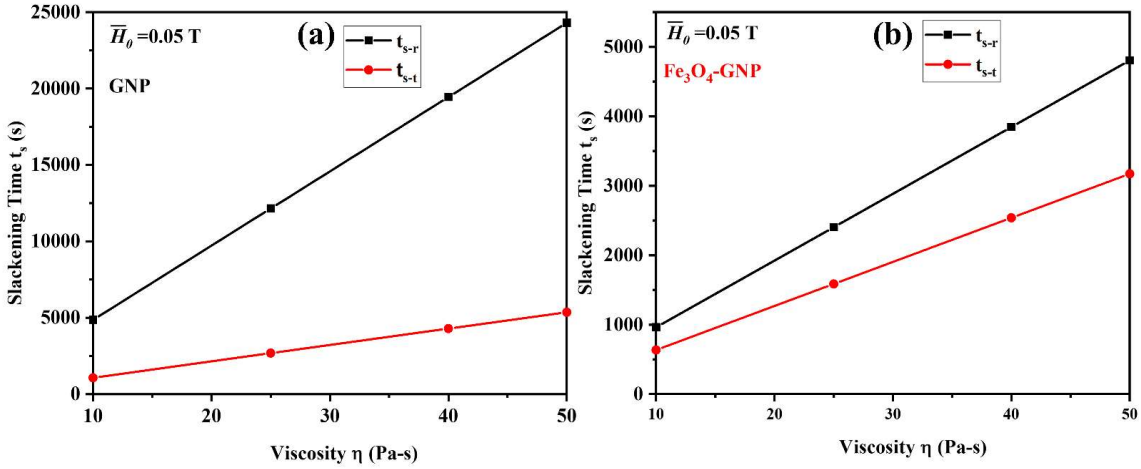

Fig. 3.14. shows the influence viscosity on the rotational and translation slackening time of (a) GNP and (b) Fe_3O_4-GNP.

3.5.5. Considerations on the model results

The characteristics for various conditions are reported in

Time (s)	$\bar{H}_0 = 0.05$ T							
	$\eta = 10$ Pa-s		$\eta = 25$ Pa-s		$\eta = 40$ Pa-s		$\eta = 50$ Pa-s	
	GNP	Fe3O4-GNP	GNP	Fe3O4-GNP	GNP	Fe3O4-GNP	GNP	Fe3O4-GNP

t_r	147636	203	367732	514	591678	820	738862	1023
t_c	19584	37	48789	95	78678	153	97857	189
t_m	322	328332	696	928389	1418	1890744	5154	7132748
$ts-r$	4818	971	12142	2430	19466	3852	24271	4785
$ts-t$	870	611	2618	1580	4258	2582	5350	3136

Table 3.3 to determine the durations of all above-described physical phenomena and to optimise the main controlling parameters i.e., applied magnetic field and viscosity of epoxy for an appropriate experimental set in the creation of complete alignments of GNP and Fe_3O_4-GNP nanoparticles. With reference to **Fig. 3.7** in later section, the gelling time for epoxy is approximately 15 minutes (900 sec). The information in

Table 3.3 shows that the total time (t_r + t_c) for rotational and chaining phenomena of Fe_3O_4-

Time (s)	$\bar{H}_0 = 0.05$ T							
	$\eta = 10$ Pa-s		$\eta = 25$ Pa-s		$\eta = 40$ Pa-s		$\eta = 50$ Pa-s	
	GNP	Fe3O4-GNP	GNP	Fe3O4-GNP	GNP	Fe3O4-GNP	GNP	Fe3O4-GNP
t_r	147636	203	367732	514	591678	820	738862	1023
t_c	19584	37	48789	95	78678	153	97857	189
t_m	322	328332	696	928389	1418	1890744	5154	7132748
$ts-r$	4818	971	12142	2430	19466	3852	24271	4785
$ts-t$	870	611	2618	1580	4258	2582	5350	3136

GNP at applied magnetic field $\bar{H}_0 = 0.05$ T for all viscosity variations of epoxy is either shorter (for $\eta = 10$ Pa-s and $\eta = 25$ Pa-s) or much larger (for $\eta = 50$ Pa-s) than the time needed for epoxy to gel (i. e. 900 s) except for the viscosity $\eta = 40$ Pa-s (Total time = t_r + t_c = 820 + 153 = 973 s $\simeq$ 900 s) which seems to be closest. Therefore, the optimised values for the applied magnetic field and viscosity are specified as $\bar{H}_0 = 0.05$ T and $\eta = 40$ Pa-s, respectively. This is because, under these ideal conditions, there are no migration or slackening effects during the alignment process of the nanoparticles and the alignments process until the chaining is completed before the gelation of epoxy.

We are fully aware that the strong van der Waals interactions are the likely cause of the GNP and Fe_3O_4-GNP carbon nanoparticles dispersed in epoxy to tend to remain in bundles rather than be split into individual platelets. A probe sonicator is used to shatter the van der Waals

bonds of the nanoparticles, although sometimes this separation may not be complete. The results of the mathematical model's correlation with the experimental data may be influenced by this.

Table 3.3. Comparison of alignment times at constant magnetic field for different viscosities of epoxy for GNP and Fe3O4-GNP nanoparticles

Time (s)	$\bar{H}_0 = 0.05$ T							
	$\eta = 10$ Pa-s		$\eta = 25$ Pa-s		$\eta = 40$ Pa-s		$\eta = 50$ Pa-s	
	GNP	Fe_3O_4-GNP	GNP	Fe_3O_4-GNP	GNP	Fe_3O_4-GNP	GNP	Fe_3O_4-GNP
t_r	147636	203	367732	514	591678	820	738862	1023
t_c	19584	37	48789	95	78678	153	97857	189
t_m	322	328332	696	928389	1418	1890744	5154	7132748
t_{s-r}	4818	971	12142	2430	19466	3852	24271	4785
t_{s-t}	870	611	2618	1580	4258	2582	5350	3136

In the mathematical model optimised parameters (magnetic field, epoxy viscosity, and time required) are evaluated to fabricate highly aligned Fe_3O_4-GNP epoxy nanocomposite with significant improvement in the functional material characterization for advanced nanocomposite base structures. Physical model of the alignment process induced by weak applied DC magnetic field was developed on GNP and Fe_3O_4-GNP suspended in epoxy.

3.6.Conclusion

A mathematical equation has been developed to describe the rotational motion of single nanoparticle under an applied magnetic field. Differential equations for the translational motion of nanoparticles, accounting for the attraction between adjoining magnetized nanoparticles has been established. It is found that the rotating contribution dominated the assembly of the nanoparticle chain as compared to translational time. The migration of magnetized nanoparticles towards the south pole is seen to be driven by the magnetophoretic mobility. Slackening mechanism of the nanoparticles is also taken into consideration in the model.

Through optimization of the processing conditions, a fully cured nanocomposite with aligned Fe_3O_4-GNP was produced, with the DC magnetic field only required close to the gel point. In conclusion, this study optimized the alignment parameters of Fe_3O_4-GNP through a mathematical model and produced a highly aligned nanocomposite using a weak DC magnetic field of 0.05 T and 40 Pa-s dynamic viscosity of epoxy.